Supplementary Information

Continuous flow hydrogenolysis of 5-hydroxymethylfurfural into 2,5-dimethylfuran over alumina-supported nickel-iron alloy catalysts

Munsuree Kalong[a], Atthapon Srifa[a,*], Sakhon Ratchahat[a], Wanida Koo-amornpattana[a], Yingyot Poo-arporn[b], Wanwisa Limphirat[b], Pongtanawat Khemthong[c], Suttichai Assabumrungrat[d,e], Keiichi Tomishige[f], Sibudjing Kawi[g]

[a] Department of Chemical Engineering, Faculty of Engineering, Mahidol University, Nakhon Pathom 73170, Thailand

[b] Synchrotron Light Research Institute, Nakhon Ratchasima, 30000, Thailand

[c] National Nanotechnology Center (NANOTEC), National Science and Technology Development Agency (NSTDA), Pathum Thani 12120, Thailand

[d] Center of Excellence in Catalysis and Catalytic Reaction Engineering, Department of Chemical Engineering, Faculty of Engineering, Chulalongkorn University, Bangkok 10330, Thailand

[e] Bio-Circular-Green-economy Technology & Engineering Center (BCGeTEC), Department of Chemical Engineering, Faculty of Engineering, Chulalongkorn University, Bangkok 10330, Thailand

[f] Department of Applied Chemistry, School of Engineering, Tohoku University, 6-6-07 Aoba, Aramaki, Aoba-ku, Sendai, 980-8579, Japan,

[g] Department of Chemical & Biomolecular Engineering, National University of Singapore, 117585, Singapore

*Corresponding authors.

Email address: atthapon.sri@mahidol.edu (A. Srifa)

Table S1 Comparison of the catalytic performance for the hydrogenolysis of 5-HMF to 2,5-DMF over the Ni-based catalysts in batch and continuous operations

Catalyst	Reactor type	Solvent	T (°C)	Time (h)	P (bar)	5-HMF conv. (%)	2,5-DMF yield (%)	Ref.
CuNi/Biochar	Batch reactor	THF	220	6	40	100	93.5	[1]
FeCoNi/h-BN	Batch reactor	THF	180	4.5	20	100	94	[2]
Co-CoO_x-FeNiCo/γ-Al_2O_3	Batch reactor	THF	190	4	10	100	99.9	[3]
Ni/ZrP	Batch reactor	THF	240	5	50	100	68.1	[4]
Ni_2In/MgO-Al_2O_3	Batch reactor	THF	200	10	10	100	93.2	[5]
NiCo	Batch reactor	THF	200	4	5	100	80.1	[6]
Ni/WO_3	Batch reactor	Water	180	6	10	>99	96	[7]
NiZnAl	Batch reactor	1,4-dioxane	180	12	15	100	93.6	[8]
NiZn	Batch reactor	2-propanol	180	4	20	100	99	[9]
NiFe/TiO_2	Batch reactor	1,4-dioxane	220	1	30	100	75	[10]
NiFe/CNT	Batch reactor	1-butanol	200	3	30	100	91.3	[11]
NiCu/ZrO_2	Continuous fixed-bed reactor (Gas phase)	1-butanol	275	WHSV=0.15 h^{-1}	15	100	70	[12]
NiCu/Carbon	Continuous fixed-bed reactor (Gas phase)	1-butanol	275	WHSV=0.15 h^{-1}	15	100	45	[13]
NiCo/Carbon	Continuous fixed-bed reactor (Liquid phases)	THF	130	WHSV=3.3 h^{-1}	10	100	>90	[14]
$Ni_{0.74}Fe_{0.97}Al$	Continuous fixed-bed reactor (Liquid phases)	Ethanol	160	WHSV=0.3 h^{-1}	40	100	90.5	This work

Table S2 Number of acidic sites obtained from the NH_3-TPD profiles of the reduced catalysts

Catalysts	Weak acidic sites (mmol NH_3/g_{cat})	Strong acidic sites (mmol NH_3/g_{cat})
Al_2O_3	0.62	1.03
FeAl	0.12	0.55
$Ni_{0.74}Fe_{0.97}Al$	0.27	1.20
NiAl	0.41	1.46

Table S3 Elemental composition and physical properties of the fresh and spent $Ni_{0.74}Fe_{0.97}Al$ catalysts

Sample	Elemental composition (%) [a]			S_{BET} [b]	V_p [c]	D_p [d]
	Fe	Ni	Al_2O_3	($m^2\ g^{-1}$)	($cm^3\ g^{-1}$)	(nm)
Fresh $Ni_{0.74}Fe_{0.97}Al$	11.9	9.5	78.6	164.2	0.37	9.2
Spent $Ni_{0.74}Fe_{0.97}Al$	11.1	9.0	79.9	157.2	0.35	9.2

[a] Elemental composition obtained from XRF measurement.

[b] S_{BET} obtained from the adsorption branch of the N_2 isotherm.

[c] V_p calculated from N_2 adsorption at a relative pressure of ~0.99.

[d] D_p obtained from the desorption branch using the BJH method.

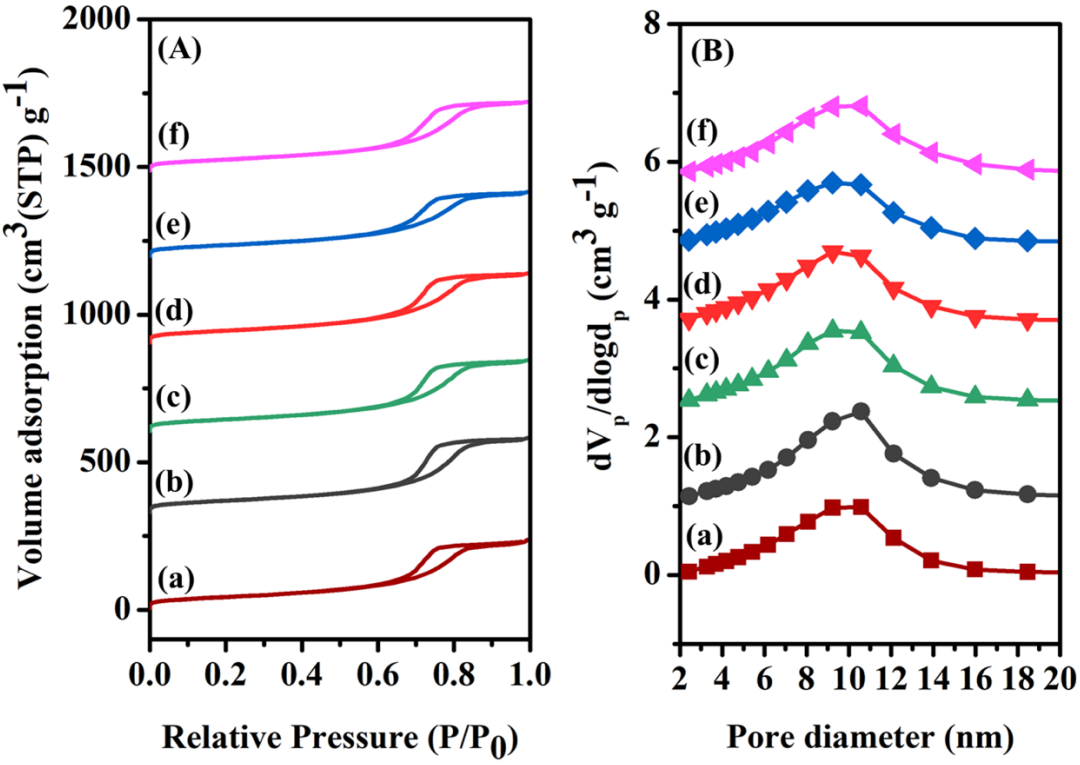

Figure S1. N_2 (A) adsorption and (B) desorption isotherms of FeAl, (b) $Ni_{0.33}Fe_{1.02}Al$, (c) $Ni_{0.56}Fe_{1.03}Al$, (d) $Ni_{0.74}Fe_{0.97}Al$, (e) $Ni_{1.04}Fe_{0.98}Al$, and (f) NiAl catalysts

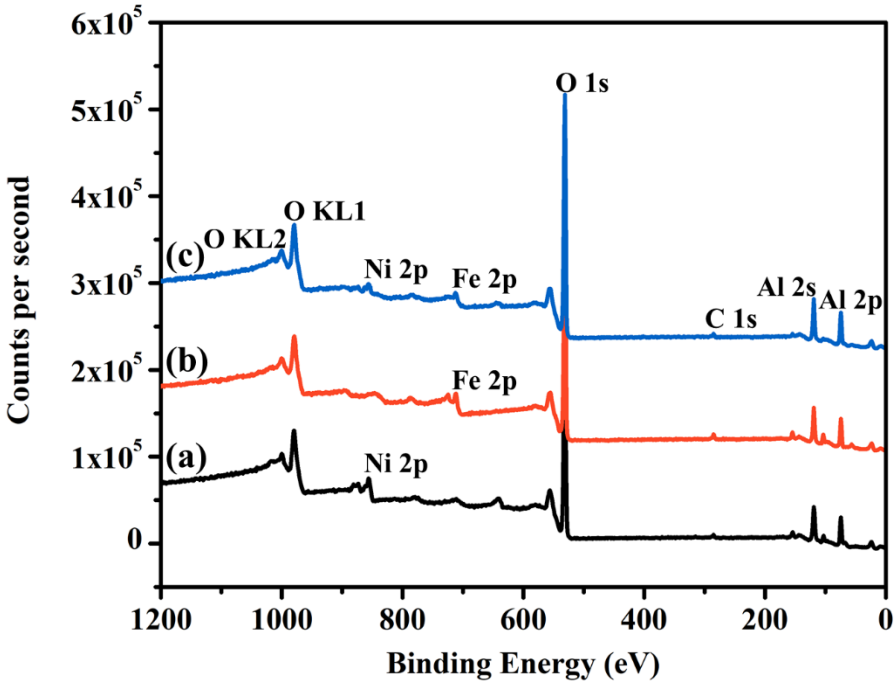

Figure S2. XPS survey of the reduced and passivated (a) NiAl, (b) FeAl, and (c) $Ni_{0.74}Fe_{0.97}Al$ catalysts

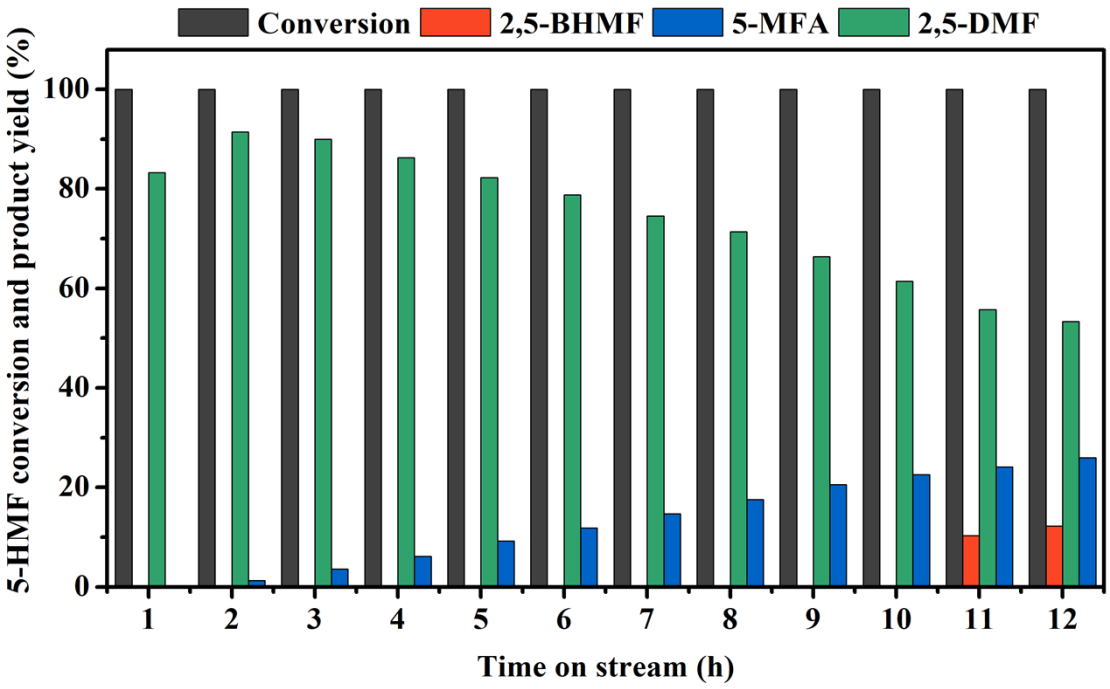

Figure S3. 5-HMF conversion and product yields on time-on-stream over $Ni_{0.74}Fe_{0.97}Al$ catalyst at a reaction temperature of 160 °C, H_2 pressure of 30 bar, and WHSV of 0.3 h^{-1}. The mole ratio of H_2 to 5-HMF was fixed at 1: 25.

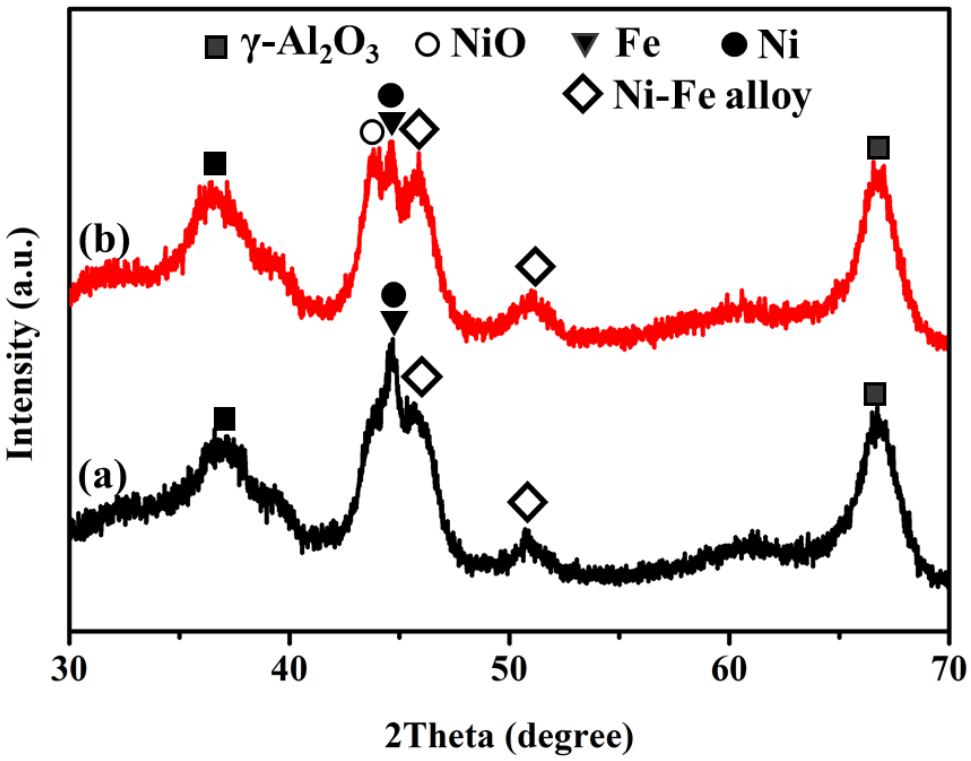

Figure S4. XRD patterns of the (a) reduced and (b) spent $Ni_{0.74}Fe_{0.97}Al$ catalysts after a reaction temperature of 160 °C, H_2 pressure of 30 bar, WHSV of 0.3 h^{-1}, and 12 h time-on-stream.

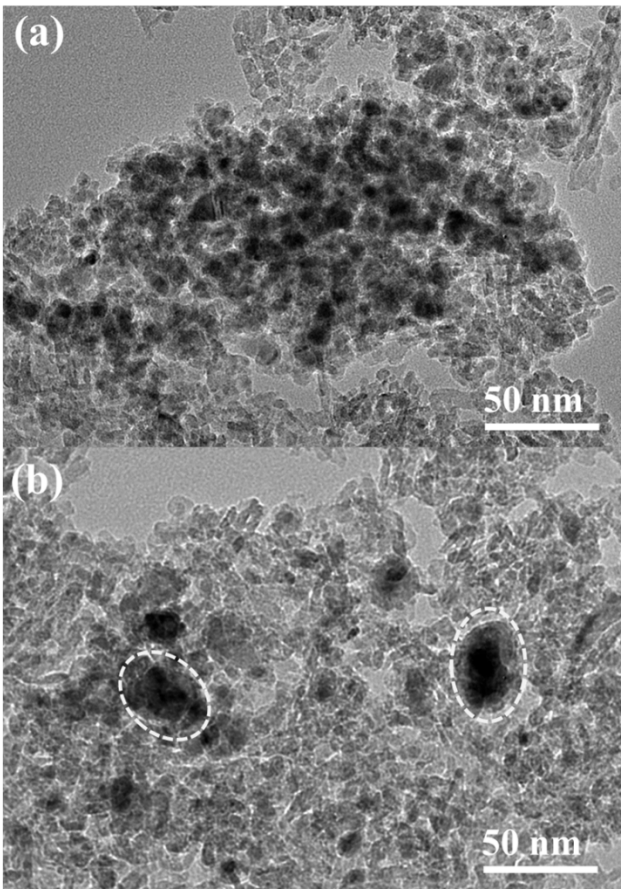

Figure S5. Typical TEM images of the (a) reduced and (b) spent $Ni_{0.74}Fe_{0.97}Al$ catalysts after a reaction temperature of 160 °C, H_2 pressure of 30 bar, WHSV of 0.3 h^{-1}, and 12 h time-on-stream.

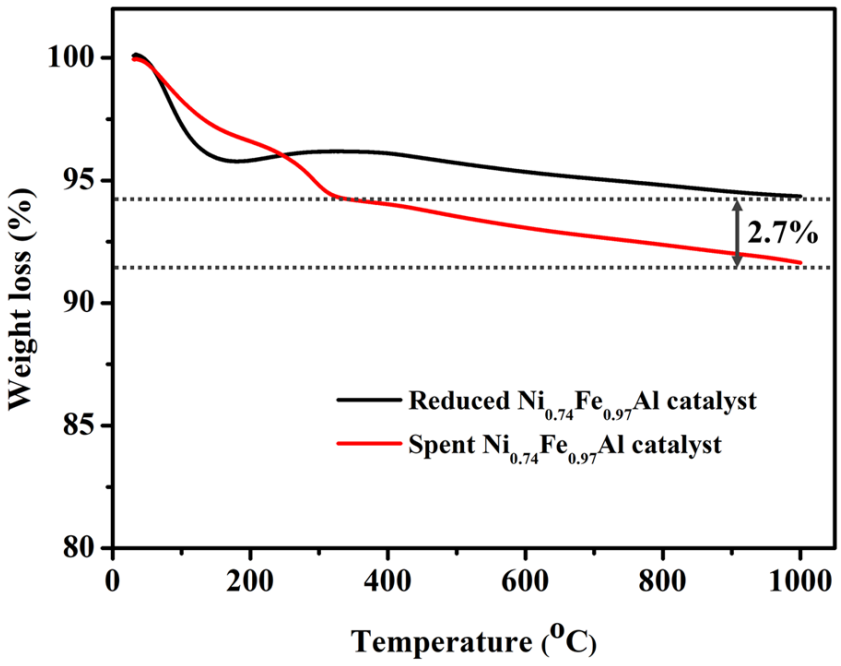

Figure S6. TGA profiles of the reduced and spent $Ni_{0.74}Fe_{0.97}Al$ catalysts after a reaction temperature of 160 °C, H_2 pressure of 30 bar, WHSV of 0.3 h^{-1}, and 12 h time-on-stream.

References

1. Y. Yang, Q. Liu, D. Li, J. Tan, Q. Zhang, C. Wang and L. Ma, *RSC Advances*, 2017, **7**, 16311-16318.
2. N. Chen, Z. Zhu, T. Su, W. Liao, C. Deng, W. Ren, Y. Zhao and H. Lü, *Chemical Engineering Journal*, 2020, **381**, 122755.
3. R. Ahishakiye, F. Wang, X. Zhang, M. Sun, Y. Zhai, Y. Liu, Y. Wu, M. Li, M. Li and Q. Zhang, *Chemical Engineering Journal*, 2022, **450**, 138187.
4. C. Zhu, Q. Liu, D. Li, H. Wang, C. Zhang, C. Cui, L. Chen, C. Cai and L. Ma, *ACS Omega*, 2018, **3**, 7407-7417.
5. Y. Li, R. Wang, B. Huang, L. Zhang, X. Ma, S. Zhang, Z. Zhu, H. Lü and K. Yang, *Applied Surface Science*, 2022, **604**, 154579.
6. W. Zhao, Z. Huang, L. Yang, X. Liu, H. Xie and Z. Liu, *Applied Surface Science*, 2022, **577**, 151869.
7. N. Siddiqui, A. S. Roy, R. Goyal, R. Khatun, C. Pendem, A. N. Chokkapu, A. Bordoloi and R. Bal, *Sustainable Energy & Fuels*, 2018, **2**, 191-198.
8. X. Kong, Y. Zhu, H. Zheng, Y. Zhu and Z. Fang, *ACS Sustainable Chemistry & Engineering*, 2017, **5**, 11280-11289.
9. W. Han, S. Wang, Y. Liu, C. Li, N. Yuan, L. Zhou, M. Tang and H. Ge, *Molecular Catalysis*, 2022, **531**, 112698.
10. M. Przydacz, M. Jędrzejczyk, J. Rogowski, M. Szynkowska-Jóźwik and A. M. Ruppert, *Energies*, 2020, **13**, 4660.
11. L. Yu, L. He, J. Chen, J. Zheng, L. Ye, H. Lin and Y. Yuan, *ChemCatChem*, 2015, **7**, 1701-1707.
12. N. Viar, J. M. Requies, I. Agirre, A. Iriondo, M. Gil-Calvo and P. L. Arias, *ACS Sustainable Chemistry & Engineering*, 2020, **8**, 11183-11193.
13. N. Viar, J. M. Requies, I. Agirre, A. Iriondo, C. García-Sancho and P. L. Arias, *Energy*, 2022, **255**, 124437.
14. P. Yang, Q. Xia, X. Liu and Y. Wang, *Journal of Energy Chemistry*, 2016, **25**, 1015-1020.